Applied Catalysis B: Environmental 144 (2014) 196–202

Contents lists available at ScienceDirect

Applied Catalysis B: Environmental

journal homepage: www.elsevier.com/locate/apcatb

Synergistic photocatalytic effect of TiO_2 coatings and *p*-type semiconductive SiC foam supports for degradation of organic contaminant

Dong Hao [a,b], Zhenming Yang [a], Chunhai Jiang [a], Jinsong Zhang [a,*]

[a] Institute of Metal Research, Chinese Academy of Sciences, Shenyang 110016, China
[b] University of Chinese Academy of Sciences, Beijing 100049, China

ARTICLE INFO

Article history:
Received 15 March 2013
Received in revised form 30 June 2013
Accepted 3 July 2013
Available online 13 July 2013

Keywords:
TiO_2–SiC
Composite sol–gel
Structured photocatalyst
Photocatalytic activity

ABSTRACT

Structured TiO_2–SiC photocatalysts were prepared by coating TiO_2 nanoparticles on Si incorporated SiC foam supports, and their photocatalytic activities toward degradation of organic contaminant under UV light irradiation were evaluated by taking 4-aminobenzenesulfonic acid (4-ABS) as a model contaminant. In comparison to SiC foam support and TiO_2 nanoparticles the TiO_2–SiC photocatalysts exhibited significantly enhanced photocatalytic performance. The effects of coating thickness of TiO_2 and pore sizes of the SiC foam supports on the photocatalytic activities were studied. A synergistic photocatalytic effect between the *p*-type semiconductive SiC foam supports and the *n*-type TiO_2 coating was proposed to account for this enhanced photocatalytic properties.

1. Introduction

Water purification has become one of the most important water related issues along with the development of modern industries and agricultures [1,2]. As one advanced oxidation technology, photocatalysis has shown great potential in water purification, especially for degradation of various organic pollutants [3–5]. TiO_2 as one of the most promising phtocatalysts has attracted special attention because of its wide band gap, non-toxicity, chemical and light stability [6,7]. However, powdery TiO_2 catalysts must be dispersed in the reaction system to improve the efficiency, which may cause easy loss of the catalyst and also difficulty in separation [8]. Therefore, immobilization of TiO_2 on various substrates, such as glass, silicon, quartz beads, activate carbon and glass fibers, has been a hot issue in recent years to assist the separation and recycling of the catalyst [9–13]. Further, it will be desirable for more rapid and efficient purification of water if a substrate can have synergistic photocatalytic effect with the TiO_2 coatings besides functioning as a support. In other words, coupling an appropriate substrate with TiO_2 coatings might be an effective way to improve the photocatalytic activity.

Silicon carbide (SiC) foam ceramics have been considered as attractive substrates for TiO_2 catalyst due to their macroporous and three-dimensionally interconnected structure, which may effectively improve the dispersion of TiO_2 and also lead to easy access of the contaminated water or air to the photocatalyst. Moreover, SiC foam ceramics own the merits of low density, large specific surface area, anti-oxidation stability, high conductivity, high temperature and corrosion resistance [14], which may enable them to be used in harsh environments with high durability. In addition, SiC foam ceramics can also be shaped into various forms to meet the requirements of different structured reactors [15–18]. In previous works, SiC foams have been successfully used as substrates for TiO_2 coatings in structured catalysts [19,20]. However, the possible synergistic photocatalytic effect of SiC foams with TiO_2 coatings has not been reported so far. In fact, as a semiconductor with a band gap of 3.0 eV, SiC has been coupled with TiO_2 nanoparticles by a few researchers to form TiO_2–SiC composite phtocatalysts [21–24]. The positive role of SiC on the enhancement of the photocatalytic property has been confirmed. For example, in a WO_3/SiC–TiO_2 system, Keller and Garin studied the photocatalytic property and explained the mechanism of SiC and TiO_2 coupled for photocatalysis [21]. They believed that the coupled SiC and TiO_2 met the requirement of classical charge-carrier transport mechanism. The photo-induced electrons can transfer from the

* Corresponding author at: Institute of Metal Research, Chinese Academy of Sciences, 72 Wenhua Road, Shenyang 110016, China. Tel.: +86 24 23971896; fax: +86 24 23971896.
E-mail address: jshzhang@imr.ac.cn (J. Zhang).

0926-3373/$ – see front matter © 2013 Elsevier B.V. All rights reserved.
http://dx.doi.org/10.1016/j.apcatb.2013.07.016

conduction band of SiC to the conduction band of TiO_2 and the holes generated on the TiO_2 valence band will transfer to the valence band of SiC. As the results, the separation of photo-induced charge carriers and photocatalytic property of the coupled nanoparticles are enhanced.

Based on this mechanism, we suppose that if the semiconductive property of the SiC foam supports can be tuned, we may not only solve the problems of dispersion and separation of TiO_2 nanoparticles, but can also obtain a structured photocatalyst with coupled SiC and TiO_2 semiconductors to enhance the photocatalytic efficiency. For this purpose, in this work, we used Si incorporated *p*-type SiC semiconductor foams as the supports and a composite sol–gel method as was developed by Barrow et al. to prepare the TiO_2 coatings [25]. The photocatalytic properties of the prepared TiO_2–SiC composite photocatalyst as well as the bare SiC foams and TiO_2 nanoparticles were compared by taking 4-aminobenzenesulfonic acid (4-ABS) as a model contaminant under UV irradiation. We confirmed that the best photocatalytic property was achieved on TiO_2–SiC composite photocatalyst. The effects of TiO_2 loadings and pore sizes of the SiC foam supports on the photocatalytic properties of the composite photocatalysts as well as the recycling of the composite photocatalysts were investigated. The possible mechanism for the coupling of TiO_2 and SiC form supports and the enhancement of the photocatalytic properties was discussed.

2. Experimental

2.1. Materials

The SiC foam ceramics were prepared by macromolecule pyrogenation method combined with reaction sintering. The detailed preparation procedure can be found in our previous work [14]. The SiC foam ceramics that have a volume fraction of 30% and pore sizes of 1.0, 1.3 and 2.5 mm respectively were shaped to flat rings of 56 mm in outer diameter, 28 mm in inner diameter and 12 mm in height, respectively. Before coating of TiO_2, the SiC foam ceramics were treated in boiling NaOH solution (10 M) for 5 min and ultrasonically cleaned with ethanol and deionized water for several times before they were dried at 120 °C for 6 h.

Tetrabutyltitanate (TBT), absolute ethanol (EtOH), aqueous hydrochloride (HCl) and 4-aminobenzenesulfonic acid (4-ABS) were purchased from Sinopharm Chemical Reagent Ltd. Co., China. Commercial titanium dioxide (TiO_2) was purchased from Nanjing High Tech. Ltd. Co., China. All chemicals were analytical grade and were used as received without any further purification. Deionized (DI) water with a resistance of 18.2 MΩ was used throughout in this study.

2.2. Preparation of TiO_2–SiC composite photocatalyst

The TiO_2 coating process was carried out by composite sol–gel method [25]. First, Ti-sol was prepared by mixing TBT, EtOH, HCl and DI water with the weight ratio of 5:15:1:5, followed by stirring for 30 min, and then standing for 3 h at room temperature. Then, TiO_2 powders were added into the Ti-sol with a weight percent of 5 wt%. The mixture was ball-milled for 1 h to get the slurry for coating. Second, the SiC foam rings were dipped into the slurry and held in it for a few minutes. After being taken out, the extra slurry in the pores of the SiC foams was blown off by using compressed air. The coated SiC foam rings were dried at 100 °C in oven. The above coating procedure was repeated for several times to achieve the expected coating mass. At last, the coated SiC foam rings were calcined at 500 °C for 1 h to convert the Ti-gel into nanometer-sized TiO_2 and finally form the TiO_2–SiC composite photocatalysts with firmly bonded TiO_2 coatings on the SiC foam supports.

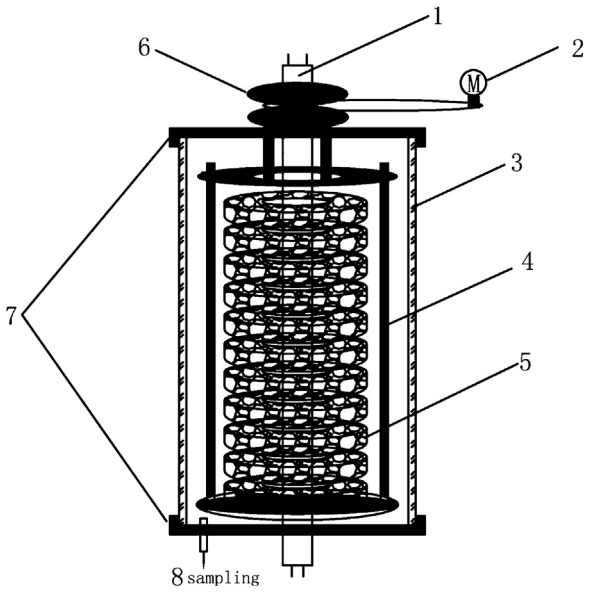

Fig. 1. Schematic diagram of the photo reactor. (1) UV lamp; (2) motor stirrer; (3) quartz tube; (4) catalyst holder; (5) TiO_2–SiC foams; (6) pulley; (7) flange; (8) sampling.

TiO_2–SiC composite photocatalysts with different pore sizes of SiC foams and loading amounts of TiO_2 were prepared. To simplify the description, the TiO_2–SiC composites with pore size of 1.3 mm and TiO_2 loading of 0.25, 0.50 and 0.75 g were marked as TSM-1, TSM-2 and TSM-3, respectively. The TiO_2–SiC composites with TiO_2 loading of 0.50 g and the pore sizes of 1.0 and 2.5 mm were denoted as TSS and TSL, respectively. The photocatalytic property of the bare SiC foams was also measured, as was named by SiC support.

2.3. Characterizations

X-ray diffraction (XRD) analysis of the TiO_2–SiC composites was performed on an X-ray Diffractometer (D/Max-2500PC) with CuK_α radiation. Microstructures of the surface and cross-section of the TiO_2–SiC composite foams were examined using a field emission scanning electron microscopy (LEO S360). The surface photovoltage of the TiO_2–SiC composite was measured by surface photovoltage spectroscopy provided by Jilin University [26].

2.4. Photocatalytic property

The photocatalytic property of the TiO_2–SiC composite foams was evaluated by degrading 4-ABS as a model contaminant under UV-light irradiation. A self-designed cylindrical quartz glass photo reactor with an inner diameter of 80 mm and height of 200 mm is shown in Fig. 1. The TiO_2–SiC foams were placed on a catalyst holder, which was connected to an electric motor so that the TiO_2–SiC foams can move around the UV-lamp (PHILIPS 8 W, with the main emission wavelength of 365 nm). A 750 mL 4-ABS solution with an initial concentration of 100 ppm was added to the reactor. During photocatalysis, 5 mL of the solution was taken after a certain time interval and subjected to liquid chromatography mass spectrometry measurements to determine the intermediate concentration of 4-ABS in the solution. Before all the experiments, the adsorption of 4-ABS by TiO_2–SiC composite foams was measured under dark condition. The concentration change of 4-ABS after reaching adsorption equilibrium was very small. Therefore, the adsorption of TiO_2–SiC was ignored in this study.

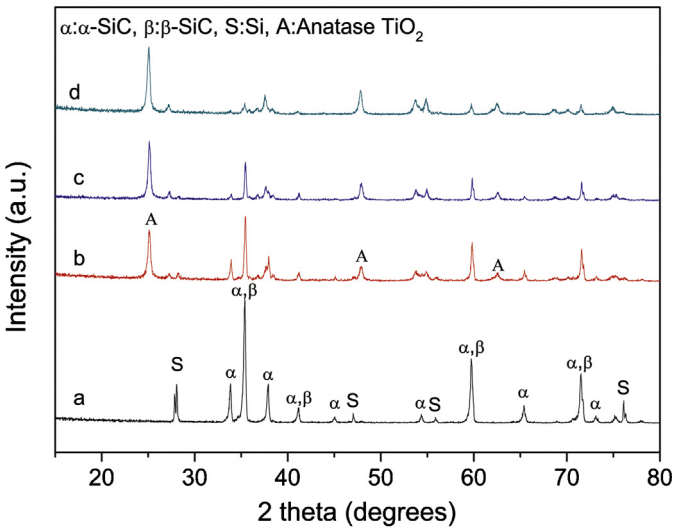

Fig. 2. X-ray diffraction patterns of (a) SiC foam and TiO_2–SiC foam photocatalysts named as (b) TSM-1, (c) TSM-2, and (d) TSM-3.

3. Results and discussion

3.1. The structure and morphology of the TiO_2–SiC foam photocatalysts

Fig. 2(a)–(d) shows the XRD spectra of the SiC foam support, TSM-1, TSM-2 and TSM-3, respectively. The SiC foam is composed of α-SiC, β-SiC and Si. The existence of residual Si in the SiC foam leads the substrate to a *p*-type semiconductor. From Fig. 2(b)–(d), we can see that the three TiO_2–SiC composite foams exhibit similar phase assemblage. The Si peak almost disappears in the composites in comparison to the bare SiC foam. The TiO_2 coating shows the typical anatase crystal structure. With the increase of TiO_2 loading, the peaks of anatase TiO_2 become stronger. Meanwhile, as the SiC is covered by anatase coating layer the peaks of α-SiC, β-SiC become weaker.

Fig. 3(a) shows the digital photos of SiC support and TiO_2–SiC composite foam (TSM-2). The dark bare SiC foam (left) is sponge-like as it was prepared from a macroporous polymer template. By using the composite sol–gel coating process, the surface of SiC foam support was completely and uniformly coated with TiO_2 (right). Fig. 3(b) and (c) shows the SEM images of the surface and cross-section of a strut of TSM-2. The TiO_2 coating layer is about 10 μm and with TiO_2 particles of approximately 10–100 nm in diameters. The distribution of TiO_2 coating over the support is continuous and homogeneous, without observable breakage. It is worthy to note that the TiO_2 coating layer is rather porous, which will be beneficial for increasing the contact area between the TiO_2 particles and the contaminated solution as well as improving the photocatalytic efficiency.

3.2. The adherence of TiO_2 coating and SiC foam supports

The first important thing that should be considered for structured catalysts is the durability and adherence between the substrate and the coating. Therefore, we first evaluated the adherence of TiO_2 coatings on the SiC foam supports by examining the mass loss of TiO_2 coatings during recycling tests. The TSS samples were used for this recycling test in degradation of 4-ABS with a concentration of 10 mg/L in the solution. The mass change and photocatalytic activity of the TiO_2–SiC composite foams were recorded

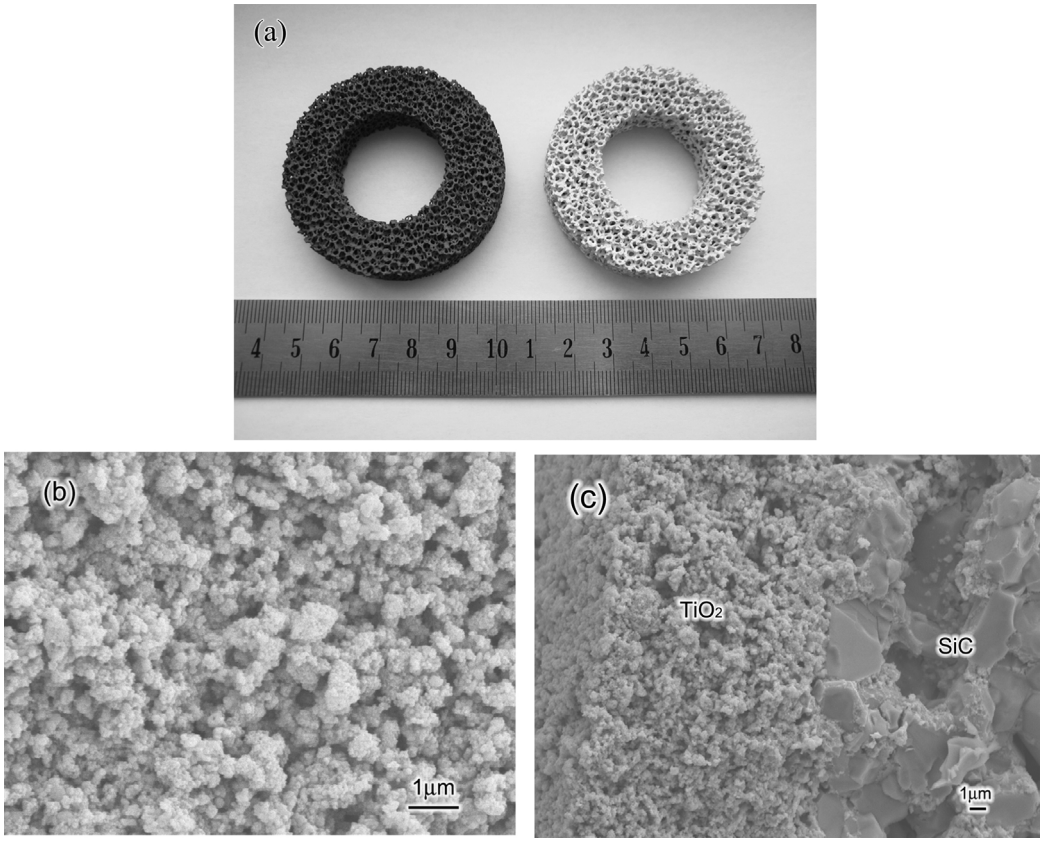

Fig. 3. (a) Digital photos of the uncoated and TiO_2 coated SiC foams, (b) surface morphology of TSM-2 and (c) cross-section morphology of TSM-2.

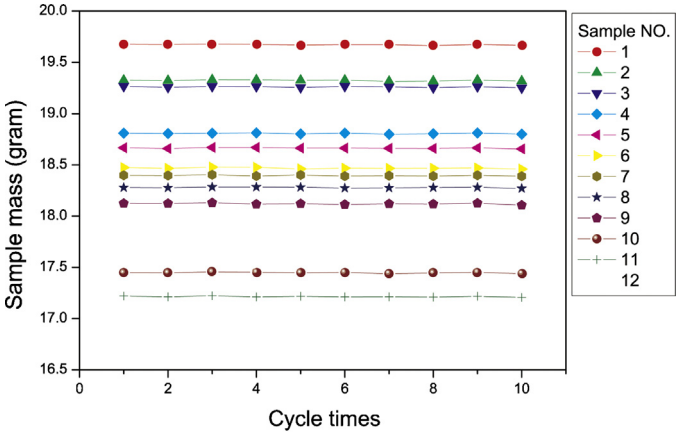

Fig. 4. Mass changes of the TiO_2–SiC photocatalyst (TSL) in ten cycles of reusing.

during each test cycle. The organic adsorbed on the TiO_2–SiC foams were burned out at 400 °C for 1 h to regenerate the photocatalysts.

As shown in Fig. 4, there was almost no mass loss with each of the 12 measured composite phtocatalysts after 10 cycles of reusing for photocatalysis experiments. This confirmed that the TiO_2 coating layer has been firmly adhered to the SiC foam supports. The degradation efficiencies of 4-ABS by TSS in the recycling tests are shown in Fig. 5. The X-axis in Fig. 5 is the degradation time in ten cycling tests. As can be seen, the TiO_2–SiC composite foam still exhibited high photocatalytic activity after ten reusing cycles though a slight drop of the degradation efficiency was observed. In other words, the TiO_2–SiC structured photocatlysts prepared in present study have manifested robust structural stability and durability for photocatalysis experiments (Section 3.3).

The photocatalytic activities of the SiC foam supports, TiO_2 nanoparticles and TSM-2 were evaluated by taking 4-ABS as a model contaminant, as shown in Fig. 6. In comparison to direct photolysis of 4-ABS, the SiC foam supports, TiO_2 nanoparticles and TSM-2 can all effectively degrade 4-ABS within 60 h. The degradation rate of TSM-2, TiO_2 and SiC foam were 100%, 62.8% and 30.9%, respectively. It was obvious that TSM-2, which was the complex of SiC and TiO_2, exhibited higher photocatalytic activity than TiO_2 nanoparticles and the SiC foam supports. The photocatalytic efficiency of TSM-2 is about 37% higher than the best efficiency of TiO_2 nanoparticles in a suspension system as was optimized in our preliminary experiments. This demonstrated that the TiO_2–SiC structured photocatalyst had not only realized the immobilization of TiO_2, but also improved the photocatalytic activity. The SiC foam support used in this work was a *p*-type semiconductor that has

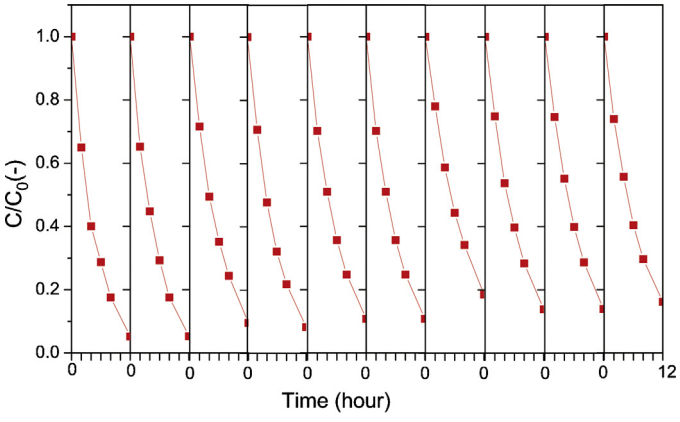

Fig. 5. Photocatalytic efficiencies of the TiO_2–SiC photocatalyst (TSL) in ten cycles of reusing.

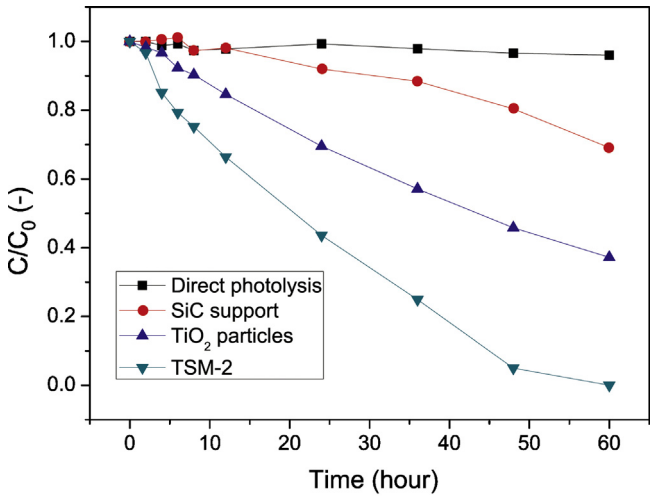

Fig. 6. Photocatalytic efficiencies of degradation of 4-ABS with direct photolysis (rectangular), SiC foam support (dot), TiO_2 particles (up-triangle) and TSM-2 (down-triangle).

photocatalysis functionality. It suggested that the SiC had acted as a modifier to TiO_2 to improve the charge separation efficiency. The possible mechanism for this enhanced photocatalytic property of the TSM system will be discussed in later section.

It should be pointed out that some organics might not be degraded completely during the photocatalysis. So it was important to test the intermediates to help to understand the photocatalytic reactions. For this purpose, the intermediate 4-ABS solutions treated by SiC foam, TiO_2 nanoparticles and structured TiO_2–SiC photocatalyst (TSM-2) were subjected to LC–MS measurements when the same 4-ABS concentration of 70 mg/L was reached (The detailed results of mass spectrometry is shown in the electronic supplementary information). It was interesting to note that when the catalyst was SiC foam, an intermediate product with molecular weight of 156 was detected (see Fig. S1). This intermediate should be the dehydroxylization product of 4-ABS after the —OH group was dehydrolized off. However, when the catalysts were TiO_2 and TSM, no intermediate product was found during the photocatalysis process (see Fig. S2). This can be ascribed to the ability of TiO_2 that can directly mineralize 4-ABS into small molecular, such as CO_2, NO_x and H_2O. As the TSM catalysts were coated with TiO_2, they can also directly mineralize 4-ABS to small molecular. Therefore, no intermediate organic product was detected (see Fig. S3).

3.3. *Effect of coating thickness on the photocatalytic activity*

It was confirmed in the above section that the structured TiO_2–SiC photocatalyst exhibited higher photocatalytic activity than TiO_2 nanoparticles and SiC foam supports. To optimize the catalytic activity of the structured photocatalyst, TSM samples with the loading amount of TiO_2 in the turn of TSM-1 < TSM-2 < TSM-3 were prepared and their photocatalytic efficiencies in degradation of 4-ABS were measured, as shown in Fig. 7. TSM-2 and TSM-1 showed the highest and lowest photocatalytic efficiencies, respectively. In the first 6 h, the degradation efficiency of TSM-3 was almost equal to that of TSM-2. But TSM-2 was more effective than TSM-3 when the reaction was proceeded further. The low efficiency of TSM-1 can be attributed to its smallest coating thickness of TiO_2, which did not fully cover the SiC foam support, so that did not provide enough active sites for the photocatalytic degradation of 4-ABS. However, besides the amount of active component, the coating thickness, i.e. the exposure rate of TiO_2 was also important to the degradation efficiency. We assumed that the best photocatalytic

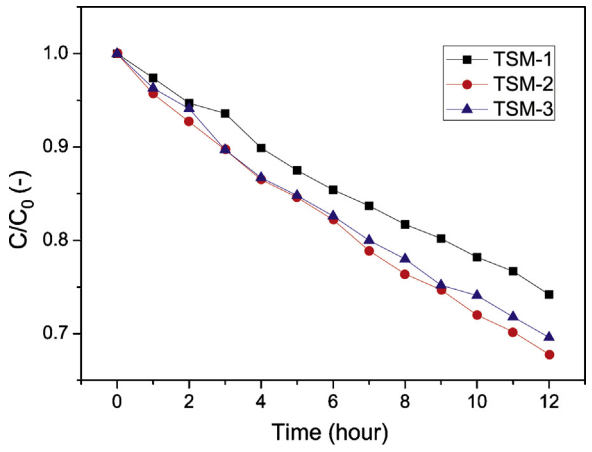

Fig. 7. Photocatalytic efficiencies of TiO_2–SiC photocatalysts with different TiO_2 loadings (The pore diameter of SiC foam is 1.3mm PPI).

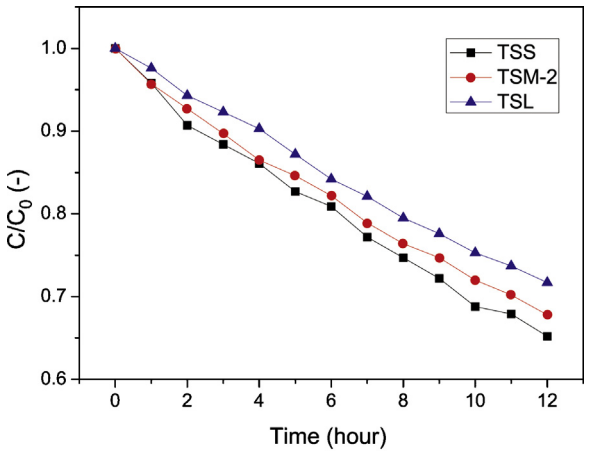

Fig. 8. Photocatalytic efficiencies of the photocatalysts TSS, TSM-2 and TSL.

efficiency could only be achieved when enough effective active components that truly take part in the photocatalytic reaction were provided. From this point of view, among the prepared TSM samples, TSM-2 was believed to fulfill best to this criterion, i.e. the optimum number of active sites had been supplied. For TSM-3, even though more TiO_2 was loaded, the severe overlapping of the TiO_2 nanoparticles might have reduced the number of active sites. In addition, the over loading of TiO_2 nanoparticles might have also reduced the synergistic photocatalytic effect between the SiC foam support and TiO_2 coating as the charge transfer was prohibited.

3.4. Effect of pore size of SiC foams on the photocatalytic activity

A higher specific surface area of the photocatalyst may favorite more adsorption of the organics onto the surface, so that to enable a more rapid photocatalytic reaction. In addition, the amount of TiO_2 exposed to UV light irradiation will also influence the photocatalytic efficiency [20]. In our research, as the pore size of the SiC foams will affect both the specific surface area and exposing rate of the photocatalyst to the UV light, the photocatalytic efficiencies of the structured photocatalysts with different pore sizes were studied. The initial pore sizes of the SiC foam for TSS, TSM-2 and TSL were 1.0, 1.3 and 2.5 mm, respectively. The surface areas of the bare SiC foam supports for these samples were estimated to be 2.112, 1.625 and 0.845 m^2, respectively. The surface area was calculated by the following equation as was proposed by Xu et al. [27].

$$a_{vs} = \frac{8.002\left(1 - 0.833\sqrt{1-\varepsilon}\right)}{d_p\sqrt{1-\varepsilon}}$$

Where ε is porosity, %, d_p is pore diameter, m, and α_{vS} is surface area of per unit volume, m^2/m^3. The TiO_2 loading of these three photocatalysts was the same, namely 0.5 g per flat ring. That means that the coating thickness of TiO_2 would be in the turn of TSS < TSM-2 < TSL. In other words, the foams with smaller pores provided higher surface area and thinner TiO_2 coating layer, which in turn supplied more active TiO_2 and also possibly more significant synergistic effect between the SiC and TiO_2 coatings for photocatalytic reaction. As shown in Fig. 8, the photocatalytic activities of these three photocatalysts were in the turn of TSS > TSM-2 > TSL, consisting with our above assumptions. Regarding the light absorption and transmission, our results showed an opposite tendency to that of Kouamé et al. [20], in which the bigger the pore size was, the higher the catalytic efficiency was obtained. The authors claimed that the higher light transmisson for the TiO_2–SiC foam photocatalyst with larger pore size had accounted for its better photocatalytic property. In our study, however, we believed that TiO_2 coating thickness, amount of active component and coupling of SiC and TiO_2 were more pronounceable to the photocatalytic property.

3.5. The synergistic photocatalytic effect of coupled TiO_2–SiC semiconductor

Coupling of semiconductors is one of the important ways to improve the photocatalytic efficiency. Heterojunctions between SiC and TiO_2 have been proposed in a few works on nano-TiO_2 coated micrometer-sized SiC particles to account for the better photocatalytic efficiency [24,28]. As shown in Fig. 3(c), the micrometer-sized SiC grains are surrounded by TiO_2 nanoparticles. That means that TiO_2–SiC Heterojunctions might have also been built by immobilization of TiO_2 nanoparticles on SiC foam support. As can be seen from the UV-visible light spectra (Fig. S4), the UV light can sufficiently penetrate the TiO_2 coating and reach the SiC support. This means that both the TiO_2 coating and SiC support can be excited by UV light irradiation and formed coupled semiconductor in the interface.

Fig. 9 schematically illustrates the flat band potentials of the valence and conduction bands at pH 1 (versus the normal hydrogen electrode (NHE)) of SiC and TiO_2 and the diagram of charge carrier transfer between TiO_2 and SiC. As we can see, the conduction band of SiC is more negative than that of TiO_2. Meanwhile, the valence band of TiO_2 is more positive than that of SiC. When SiC and TiO_2 are excited by UV light, the electrons that get to the SiC

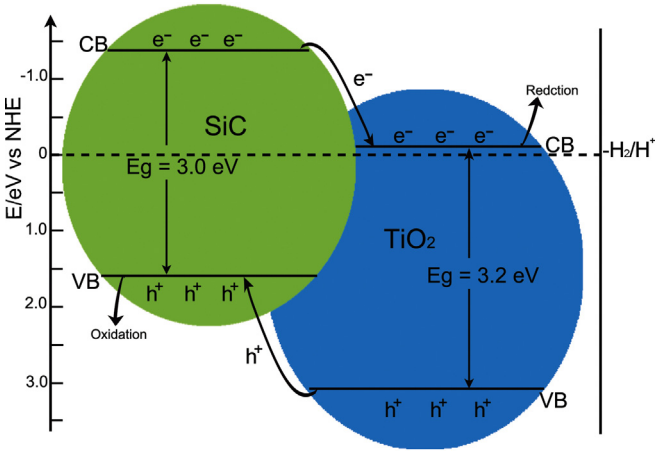

Fig. 9. Diagram of electron transfer of the coupled TiO_2–SiC semiconductor.

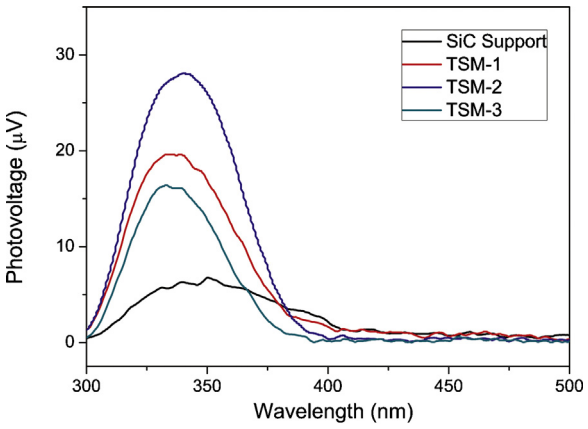

Fig. 10. The SPS spectra of SiC support and TiO_2–SiC.

conduction band will transfer from SiC to TiO_2. At the meanwhile, the holes will transfer from the valence band of TiO_2 to that of SiC. This is called classical charge transfer mechanism. Keller and Garin [21] studied the coupling effect of SiC and TiO_2 in a ternary system [21]. Other coupled semiconductors, such as WO_3–TiO_2, CdS–TiO_2, SnO_2–TiO_2, and so on, have also been investigated based on powdery samples [29–31]. In this study we demonstrated that coupling of SiC foam support and TiO_2 coatings might have also led to charge transfer between them during photocatalysis and as a result high photocatalytic activity as compared to TiO_2 nanoparticles.

Surface photovoltage spectroscopy (SPS) is a powerful tool for characterization of the surface state. In this study we cannot directly measure the surface photovoltage of the foam samples. Instead, SiC bulks with the dimension of 20 mm × 10 mm × 1 mm were prepared by the same method as that for SiC foam. The SiC bulks were then coated with the same thicknesses of TiO_2 as that for TSM-1, TSM-2 and TSM-3, respectively. The SPS spectra of the SiC bulk support and TiO_2–SiC composites with different TiO_2 loadings were compared in Fig. 10.

In the UV region (wavelength <400 nm), all samples can be excited. In comparison to the SiC support, the SPS spectrum of TiO_2–SiC was first enhanced by increasing the TiO_2 loading. However, further increasing the thickness of TiO_2 coating layer resulted in decreased intensity of the SPS spectrum. As SPS response peak reflects the net charge accumulated on the materials surface [32,33], the intensity change of the SPS spectra can be directly linked to the efficiency of charge transfer and separation. From Fig. 10 we know that overloading of TiO_2 on SiC support will decrease the charge transfer and separation between them, which is consistent with the photocatalytic efficiencies as shown in Fig. 7. In fact, Takahashi et al. [34] and Yu et al. [35] have found the similar relation between the film thickness and the ability of photo-induced charge separation. They both declared that if the film thickness were higher than the proper thickness, the charge separation ability of the heterojuctions would be decreased.

To further illustrate the synergetic effect between the *p*-type SiC substrate and the TiO_2 coating on the enhanced photocatalytic property, we systematically investigated the influence of semiconductivity of SiC foam supports on the photocatalytic efficiency of the structured photocatalyst. The experimental results showed that the TiO_2 coatings immobilized on *p*-type semiconductive SiC foam supports, namely TSM-2, exhibited obviously higher photocatalytic activity in comparison to that coated on *n*-type SiC foam support. Further, the composite structural photocatalysts made from *p*-type SiC supports but with Si containing surface or SiO_2 surface exhibited lower photocatalytic efficiency than TSM-2 but higher photocatalytic efficiency than the one made from *n*-type SiC support. This clearly indicated that the amount of *p*-type SiC that may have synergetic effect with TiO_2 coating has played a crucial role on the photocatalytic property of the composite. As we have carefully controlled the TiO_2 coating on different SiC foam supports with by same thickness and loading amount, the influence of the physical and chemical properties of the TiO_2 coatings can therefore be minimized, which ensured that the measured different photocatalytic properties can be attributed to the effect of the different substrates.

In addition, from the surface photovoltage spectra (SPS) of the SiC–TiO_2 composites made of dense flat composite but with different types of semiconductivity, we can also clearly observe stronger SPS response in the *p*-type SiC supported TiO_2 than the *n*-type SiC supported sample. This further demonstrated that the *p*-type SiC support must have a synergetic effect with the *n*-type TiO_2 coating in enhancing the photocatalytic property of the composite. The relevant study has been reported in another paper [36].

4. Conclusion

The structured TiO_2–SiC photocatalysts prepared by a composite sol–gel method exhibited efficient photocatalytic degradation of 4-ABS. The TiO_2 coating was uniform and bonded to the SiC foam support firmly as was confirmed by recycling tests. The TiO_2–SiC showed advantageous photocatalytic performance as compared to TiO_2 nanoparticles. The photocatalytic activity was highly dependent on the coating thickness of TiO_2 and pore sizes of the SiC foam supports. We believe that the coupling of the *p*-type semiconductive SiC foam supports with the *n*-type TiO_2 coating might have played important role on the photocatalytic reactions. This study also provides a solution for enhancing the photocatalytic activity of structured photocatalyst exited by visible light.

Acknowledgement

This research is supported by the National Key Technology R&D Program of China with Grant No. 2011BAE03B07. The authors would also like to thank Prof. Dejun Wang and Mr. Liping Chen for their help with the SPS experiments.

Appendix A. Supplementary data

Supplementary data associated with this article can be found, in the online version, at http://dx.doi.org/10.1016/j.apcatb.2013.07.016.

References

[1] M.A. Eltawil, Z. Zhengming, L. Yuan, Renewable and Sustainable Energy Reviews 13 (2009) 2245–2262.
[2] H. Dong, Y. Geng, J. Sarkis, T. Fujita, T. Okadera, B. Xue, Science of The Total Environment 442 (2013) 215–224.
[3] M.N. Chong, B. Jin, C.W.K. Chow, C. Saint, Water Research 44 (2010) 2997–3027.
[4] K. Nakata, A. Fujishima, Journal of Photochemistry and Photobiology C: Photochemistry Reviews 13 (2012) 169–189.
[5] T. Ochiai, A. Fujishima, Journal of Photochemistry and Photobiology C: Photochemistry Reviews 13 (2012) 247–262.
[6] A.L. Linsebigler, G. Lu, J.T. Yates, Chemical Reviews 95 (1995) 735–758.
[7] M.R. Hoffmann, S.T. Martin, W. Choi, D.W. Bahnemann, Chemical Reviews 95 (1995) 69–96.
[8] J.A. Byrne, B.R. Eggins, N.M.D. Brown, B. McKinney, M. Rouse, Applied Catalysis B: Environmental 17 (1998) 25–36.
[9] K. Hofstadler, R. Bauer, S. Novalic, G. Heisler, Environmental Science and Technology 28 (1994) 670–674.
[10] A. Fernandez, G. Lassaletta, V.M. Jimenez, A. Justo, A.R. GonzalezElipe, J.M. Herrmann, H. Tahiri, Y. AitIchou, Applied Catalysis B: Environmental 7 (1995) 49–63.
[11] X.J. Wang, Z.H. Hu, Y.J. Chen, G.H. Zhao, Y.F. Liu, Z.B. Wen, Applied Surface Science 255 (2009) 3953–3958.
[12] S. Gelover, P. Mondragón, A. Jiménez, Journal of Photochemistry and Photobiology A: Chemistry 165 (2004) 241–246.
[13] H. Hu, W.J. Xiao, J. Yuan, J.W. Shi, M.X. Chen, G.W.F. Shang, Journal of Environmental Sciences: China 19 (2007) 80–85.

[14] W. Wei, X.-m. Cao, C. Tian, J.-s. Zhang, Microporous and Mesoporous Materials 112 (2008) 521–525.
[15] Y. Jiao, C. Jiang, Z. Yang, J. Zhang, Microporous and Mesoporous Materials 162 (2012) 152–158.
[16] Z.M. Yang, J.S. Zhang, X.M. Cao, Q. Liu, Z.J. Xu, Z.M. Zou, Applied Catalysis B: Environmental 34 (2001) 129–135.
[17] G. Winé, J.-P. Tessonnier, S. Rigolet, C. Marichal, M.-J. Ledoux, C. Pham-Huu, Journal of Molecular Catalysis A: Chemical 248 (2006) 113–120.
[18] T.T. Nguyen, L. Burel, D.L. Nguyen, C. Pham-Huu, J.M.M. Millet, Applied Catalysis A: General 433–434 (2012) 41–48.
[19] N.A. Kouamé, D. Robert, V. Keller, N. Keller, C. Pham, P. Nguyen, Catalysis Today 161 (2011) 3–7.
[20] N. Kouamé, D. Robert, V. Keller, N. Keller, C. Pham, P. Nguyen, Environmental Science and Pollution Research 19 (2012) 3727–3734.
[21] V. Keller, F. Garin, Catalysis Communications 4 (2003) 377–383.
[22] H. Yamashita, Y. Nishida, S. Yuan, K. Mori, M. Narisawa, Y. Matsumura, T. Ohmichi, I. Katayama, Catalysis Today 120 (2007) 163–167.
[23] Y. Li, Z. Yu, J. Meng, Y. Li, International Journal of Hydrogen Energy 38 (2013) 3898–3904.
[24] T. Zou, C. Xie, Y. Liu, S. Zhang, Z. Zou, S. Zhang, Journal of Alloys and Compounds 552 (2013) 504–510.
[25] D.A. Barrow, T.E. Petroff, M. Sayer, Surface and Coatings Technology 76–77 (1) (1995) 113–118.
[26] T. Jiang, T. Xie, Y. Zhang, L. Chen, L. Peng, H. Li, D. Wang, Physical Chemistry Chemical Physics 12 (2010) 15476–15481.
[27] W. Xu, H. Zhang, Z. Yang, J. Zhang, Chemical Engineering Journal 140 (2008) 562–569.
[28] C. Gómez-Solís, I. Juárez-Ramírez, E. Moctezuma, L.M. Torres-Martínez, Journal of Hazardous Materials 217–218 (2012) 194–199.
[29] K.K. Akurati, A. Vital, J.-P. Dellemann, K. Michalow, T. Graule, D. Ferri, A. Baiker, Applied Catalysis B: Environmental 79 (2008) 53–62.
[30] L. Wu, J.C. Yu, X. Fu, Journal of Molecular Catalysis A: Chemical 244 (2006) 25–32.
[31] K. Vinodgopal, I. Bedja, P.V. Kamat, Chemistry of Materials 8 (1996) 2180–2187.
[32] J. Cao, J. Sun, G. Shi, H. Chen, Q. Zhang, D. Wang, M. Wang, Materials Chemistry and Physics 82 (2003) 44–48.
[33] K. Liu, J. Zhang, H. Gao, T. Xie, D. Wang, Journal of Alloys and Compounds 552 (2013) 299–303.
[34] M. Takahashi, K. Tsukigi, T. Uchino, T. Yoko, Thin Solid Films 388 (2001) 231–236.
[35] H. Yu, X. Quan, S. Chen, H. Zhao, Y. Zhang, Journal of Photochemistry and Photobiology A: Chemistry 200 (2008) 301–306.
[36] D. Hao, Z. Yang, C. Jiang, J. Zhang, Journal of Materials Science and Technology (2013) (in press).